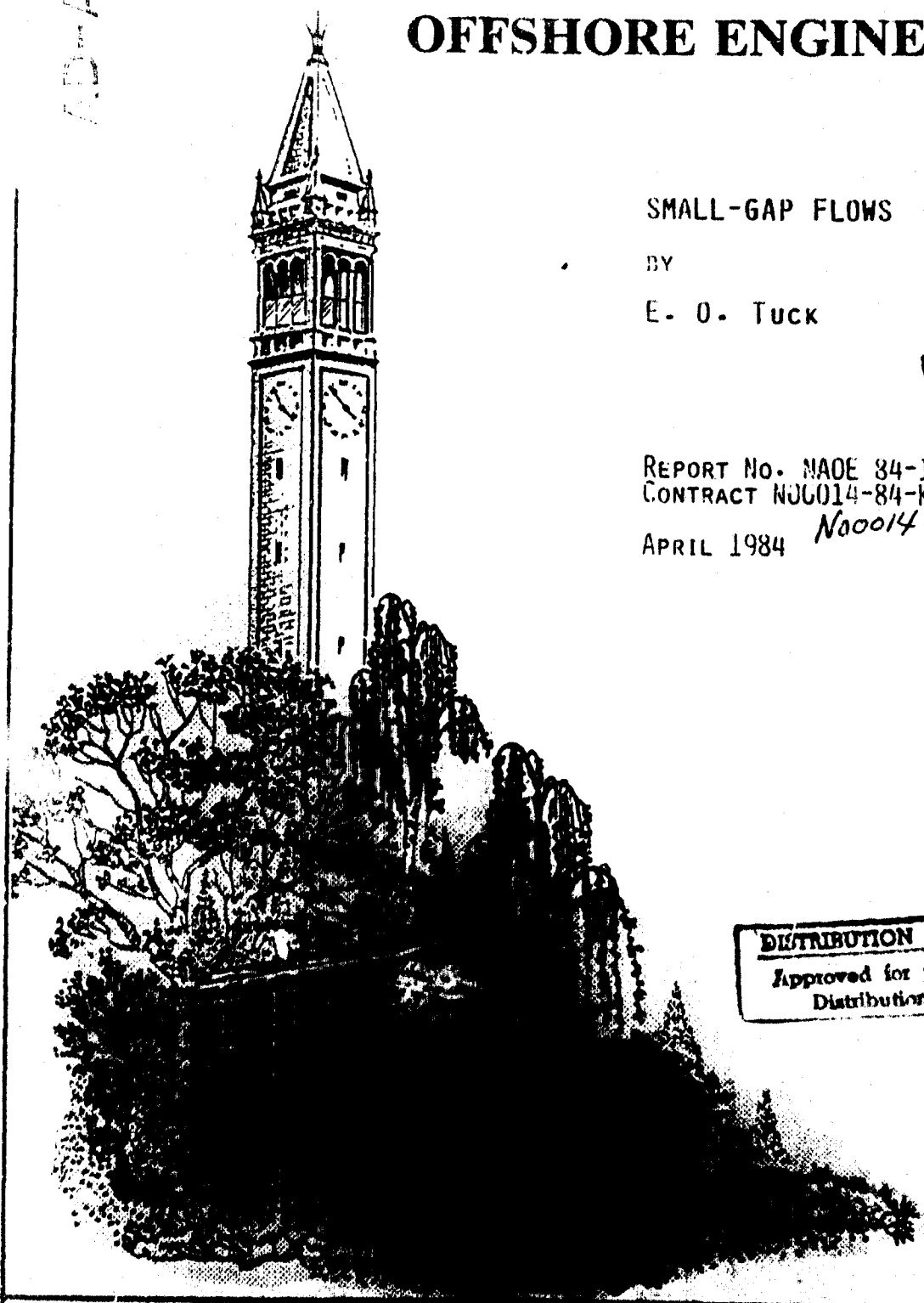


AD-A202 876

UNIVERSITY OF CALIFORNIA



# DEPARTMENT OF NAVAL ARCHITECTURE & OFFSHORE ENGINEERING



SMALL-GAP FLOWS

BY

E. O. Tuck

**SDTIC**  
**ELECTE**  
NOV 30 1988  
**S** **D**  
E

REPORT No. NAOE 84-1

CONTRACT N00014-84-K-0026

APRIL 1984

*N00014-82-K-0335*

**DISTRIBUTION STATEMENT A**  
Approved for public release  
Distribution Unlimited

UNIVERSITY OF CALIFORNIA, BERKELEY, CA 94720

88 11 30 131

(415) 642-5464

SMALL-GAP FLOWS

BY

E. O. Tuck

REPORT No. NAUE 84-1  
CONTRACT N00014-84-K-0026

APRIL 1984

REPRODUCTION IN WHOLE OR IN PART IS PERMITTED  
FOR ANY PURPOSE OF THE UNITED STATES GOVERNMENT.  
APPROVED FOR PUBLIC RELEASE; DISTRIBUTION UNLIMITED.

DEPARTMENT OF NAVAL ARCHITECTURE AND OFFSHORE ENGINEERING  
UNIVERSITY OF CALIFORNIA  
BERKELEY, CALIFORNIA 94720

## Preface

This report consists of five chapters, namely:

1. Airfoils in Extreme Ground Effect, pp. 2-6.
2. Automobile Aerodynamics, pp. 7-11.
3. Shallow-water Waves at Discontinuities; pp. 12-16.
4. Sliding Sheets, pp. 17-20.
5. Wings Over Water, pp. 21-24.

These chapters are independent of each other, although linked by the "small-gap" theme. Chapters 1-4 were originally presented in the form of a lecture series in the Department of Naval Architecture and Offshore Engineering, University of California at Berkeley, during February and March 1984. Chapter 5 formed the basis for a presentation to the panel H5 (Analytical Ship-Wave Relations) of the Society of Naval Architects and Marine Engineers, on March 20th, 1984.

Research for and preparation of this report was carried out during a period spent by the author in the Department of Mathematics, Stanford University, January-May 1984, sponsored by the Office of Naval Research under a contract to Professor Joseph B. Keller. Computing support at Stanford was provided by the CLASSiC Project, funded by the Office of Naval Research under Contract ONR N<sup>000</sup>14-82-K-0335 of Professors J. Olinger and J. Ferziger. The lecture series at U.C. Berkeley was supported by the Office of Naval Research Special Program for Ship Hydrodynamics, under contract N00014-84-K-0026, to Professor Ronald W. Yeung.

In view of the involvement of the author with both U.C. Berkeley and Stanford during the time of its preparation, this report is being issued in identical form, under separate covers of both institutions.



<b>Accession For</b>	
NTIS GRA&I	<input checked="" type="checkbox"/>
DTIC TAB	<input type="checkbox"/>
Unannounced	<input type="checkbox"/>
Justification	
By _____	
Distribution/	
Availability Codes	
Dist	Avail and/or Special
A-1	

## 1. Airfoils in Extreme Ground Effect

In this chapter, I shall concentrate on two-dimensional irrotational flows of an inviscid incompressible fluid about a thin airfoil, as in Figure 1-1. The airfoil is very close to an impermeable plane wall, and the flow is in the first instance taken to be steady.

How close is "very close"? Suppose  $\epsilon$  is a measure both of the airfoil's thinness and of its angle of attack, i.e., if  $L$  is its length, its thickness is  $O(\epsilon)L$ , and its angle of attack is  $O(\epsilon)$ . Then we assume that the clearance or gap size  $h$  is also  $O(\epsilon)L$ . That is, all points of the airfoil surface, top and bottom, are not more than  $O(\epsilon)L$  from the wall.

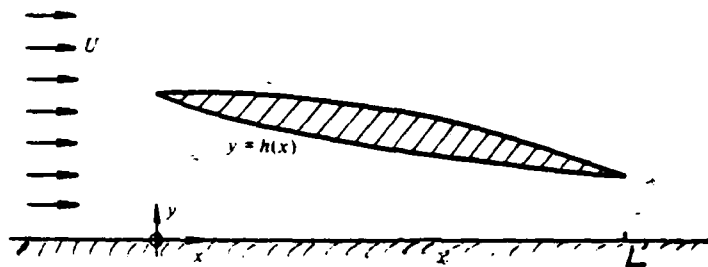


Figure 1-1. Sketch of flow situation.

This domain of closeness is indeed "very close", in comparison with the case when  $h = O(L)$ , for example. The aerodynamic problem of  $h = O(L)$  ground effect is very interesting, and deserves a chapter to itself. In that domain, significant (but not overwhelming) flow changes occur, relative to the case of an airfoil alone in an infinite fluid, and mathematical and computational difficulties involving numerical solution of singular integral equations have to be overcome before solutions can be obtained (see eg. Tuck and Newman, 1974). We say no more about that case here.

In the case of present interest,  $h = O(\epsilon)L$ , the ground-effect phenomenon is "extreme", in the sense that aerodynamic effects occur due to the presence of the wall that are much greater than those that occur in the absence of the wall; specifically, by a factor  $O(\epsilon^{-1})$ . For example, the lift on a thin airfoil at  $O(\epsilon)$  angle of attack is of  $O(\epsilon)$ , whereas the lift is  $O(1)$  in the extreme ground effect case.

How can this be, when every facet of the surface of the airfoil is placed at only a small  $O(\epsilon)$  angle to the incident stream? If the wall were not present, such a body would cause an  $O(\epsilon)$  disturbance to the stream, leading to  $O(\epsilon)$  pressure changes and hence the usual  $O(\epsilon)$  lift force.

Indeed, this is still true almost everywhere, and leads to an important conclusion. In particular, the flow over the top of the airfoil is still an  $O(\epsilon)$  disturbance to a uniform stream, and does lead to  $O(\epsilon)$  contributions to the lift. If we wished to solve the problem to an  $O(\epsilon)$  level of accuracy (ie. to find  $O(1) + O(\epsilon)$  contributions to lift, consistently) then we should need to compute the  $O(\epsilon)$  disturbance to the stream over the top of the airfoil.

But our sights are set somewhat lower (?). We are here content with the  $O(1)$  lift contributions, and hence shall neglect all  $O(\epsilon)$  contributions. This has a remarkable immediate effect, namely that we can assume that, as far as the flow above the airfoil is concerned, the airfoil doesn't exist! That is, this flow, to a consistent order of accuracy, may be taken as an undisturbed uniform stream of magnitude  $U$ . Even more important is the corollary that the pressure  $p$  in the flow above the airfoil is unchanged from the ambient value  $p_\infty$  at infinity.

So much for the flow above the airfoil. However, some fluid may pass between the airfoil and the wall. Unless the lower surface of the airfoil is exactly parallel to the wall everywhere, this fluid will be moving in a channel of variable cross-section, and hence its velocity will be non-uniform. Not only non-uniform, in fact, but in general varying significantly as the local gap width changes. That is, we must expect  $O(1)$  flow and pressure variations in the gap, and this is what leads to the  $O(1)$  net lift, discussed above.

I did say that some fluid "*may*" pass beneath the airfoil, not "*must*". Indeed, the main issue is to decide just how much fluid does so pass. The answer is not the obvious one that the airfoil "*scoops*" up those streamlines that would have passed beneath it if it had not been there. What does decide this issue?

The answer is that *trailing-edge* conditions decide it. The flow must detach smoothly from the trailing edge, and the usual Kutta condition of aerodynamics demands that the pressure be continuous across the trailing edge. But, given our consistent  $O(1)$  analysis, with the conclusion that the above-airfoil pressure is equal to ambient, this means that the trailing-edge value of the under-airfoil pressure must also be ambient. This then demands that the fluid velocity in the gap must return to the free-stream value at the trailing edge.

Suppose for example, that the airfoil was acting as a simple scoop, as above. In that case, the velocity at the *leading* edge would be continuous, and, since we have assumed that the velocity takes the free-stream value outside the gap region, this would imply that the leading-edge value of the velocity in the gap was also of the free-stream value. This fluid would then change its velocity significantly as it moved along the gap, and, in particular would emerge at the trailing edge with a velocity that is in general not equal to the free-stream value. This is not permitted; hence the scoop concept is wrong, and we must allow a discontinuity in the flow velocity at the leading edge.

That is, somehow the leading edge knows what the trailing edge is doing, and selects exactly the right amount of fluid to enter, so that free-stream conditions will prevail at the trailing edge. This "*selection*" process involves a rapid change in velocity at the leading edge, since the velocity just *ahead* of the leading edge is necessarily (with  $O(\epsilon)$  error, as usual) equal to the free-stream value.

This situation is in fact not unusual in aerodynamics, just more extreme in its consequences in the present case. The Kutta trailing-edge requirement always performs a selection process among a family of theoretically-feasible flows. In unbounded two-dimensional aerodynamics, selection occurs via a choice of the circulation about the airfoil. The present situation is no different in that respect; differing strengths of the leading-edge velocity discontinuity represent (indeed are proportional to) differing values of the circulation about the airfoil. In practice, the flow must adjust itself in an unsteady manner, if, for example it is started from rest, until the Kutta condition is satisfied in steady flow. This unsteady development, to which I return below, involves in the extreme ground-effect case, a change from an initially continuous velocity at the leading edge to the correct value of the apparent step discontinuity.

Of course there is no actual discontinuity. If we were to examine a region of characteristic dimension  $O(\epsilon).L$  located close to the leading edge, we should find a rapid but not instantaneous change from free stream to a different uniform velocity. The flow in this leading-edge neighbourhood is indeed very interesting and readily calculable by conformal mapping (see eg. Tuck and Bentwich 1983), since the boundaries can be assumed locally plane. This local flow contains the necessary leading-edge stagnation point, which lies at a distance  $O(\epsilon).L$  from the leading edge, on the airfoil's surface either above or below it, as in Figure 1-2.

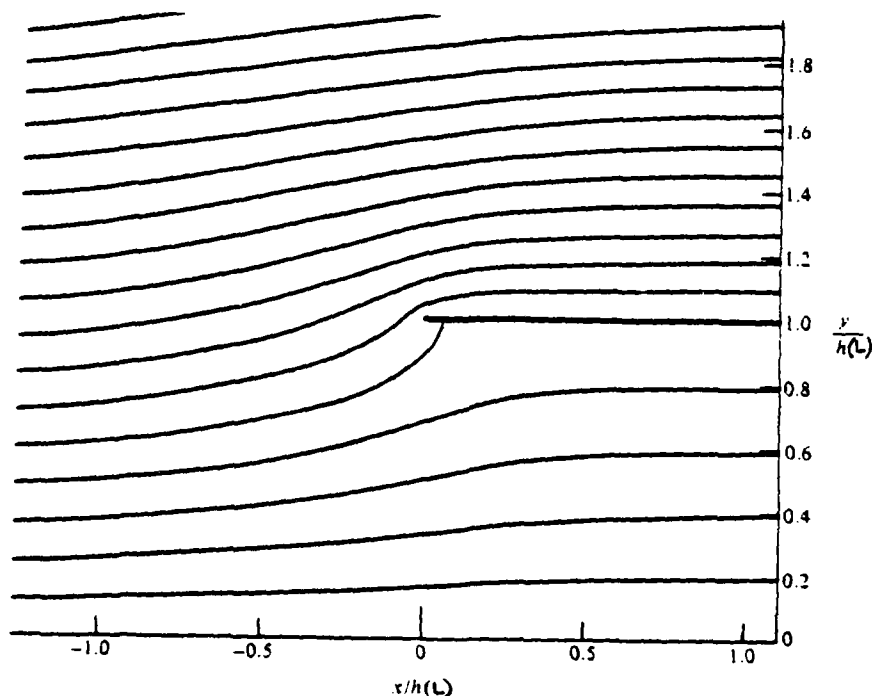


Figure 1-2. Entrance-region streamlines.

Upstream of the leading edge (locally) there is an apparent source which models rejection of some fluid particles that otherwise would have been "scooped"; the source is negative in strength, i.e. becomes a sink, if an excess of fluid above the scoop value is demanded. Downstream of the leading edge, the local flow asymptotes to a uniform stream, of exactly the right magnitude  $u(0)$  to (eventually) satisfy the Kutta condition; Figure 1-2 is drawn for the special case  $u(0) = U/2$ .

The action then takes place in the gap itself. What action? That depends on the geometry of the gap, and on the properties of the fluid. In the case of interest here, the answer is very simple, and the result is essentially Venturi's law for one-dimensional flow.

That is, if  $h = h(x)$  is the clearance or gap thickness between the lower surface of the airfoil and the wall at station  $x$  measured along the length, then the flow is one-dimensional, with a velocity  $u = u(x)$  such that  $u(x) \cdot h(x)$  is constant. Since the Kutta condition demands that  $u(L) = U$ , this "constant" is determined as  $U \cdot h(L)$ , and thus  $u(x) = U h(L) / h(x)$ . Hence the pressure coefficient is  $C_p(x) = (p - p_\infty) / (\frac{1}{2} \rho U^2) = 1 - h(L)^2 / h(x)^2$ . If, as discussed above, we assume  $p = p_\infty$ , i.e.  $C_p = 0$ , in the flow above the airfoil, the net lift per unit span is just  $F = \frac{1}{2} \rho U^2 \int C_p(x) dx$ , and the centre of pressure is at  $\bar{x} = \int x C_p(x) dx / \int C_p(x) dx$ , where  $C_p(x)$  is given above. The problem is now completely solved, given  $h(x)$ .

It is of interest to indicate the extremes of the present results. Thus  $C_p(x) \leq 1$  necessarily, so  $F \leq \frac{1}{2} \rho U^2 L$ ; i.e. the lift coefficient is less than unity, as of course it always must be in aerodynamics. However (in contrast to the unbounded-fluid case, where  $F \ll \frac{1}{2} \rho U^2 L$ ), in extreme ground effect,

a lift coefficient close to unity is (at least in theory) achievable, simply by letting  $h(L)$  vanish. That is, if we allow the trailing edge almost to touch the ground (while keeping  $h(x)$  still significantly greater than zero at all points ahead of the trailing edge), then stagnation conditions will apply over most of the gap, and hence the full stagnation pressure will be felt on the under-side of the airfoil. Of course, the velocity must return to the free stream value  $U$  at the actual trailing edge, but the net flux through the trailing-edge gap tends to zero with  $h(L)$ .

At the other extreme, an arbitrarily-large downward force (negative lift) is theoretically feasible, by allowing  $h(x)$  to vanish for some point  $x$  ahead of the trailing edge, while maintaining  $h(L) > 0$ . Again, this is physically obvious, for if a finite flux through the trailing edge is required, and if  $h(x)$  is small at one other point, then a large velocity is needed at that point, which gives a large *negative* pressure and lift.

These considerations and others are illustrated (see Figure 1-3) by computing the net lift  $F$  and centre of pressure  $\bar{x}$  for a flat plate at a constant angle of attack, as in Tuck, 1981. Various static stability results can be deduced from the behaviour of the centre of pressure as a function of angle of attack. Note that, for small angle of attack, such that  $h(x)/h(L) \approx 1$  everywhere (cf. Widnall and Barrows 1970), one can linearise the theory, and it is then easy to see that the centre of pressure is at the one-third chord point. The curves of Figure 1-3 for  $\sigma = 1$  are relevant to the present discussion; those for  $\sigma$  values other than unity correspond to an interesting attempt (Tuck 1981) to account for trailing-edge protuberances, like rudders. The parameter  $\theta$  used in Figure 1-3 is a scaled angle of attack; the related parameter  $\lambda$  is the contraction ratio, ie. trailing clearance/leading clearance.

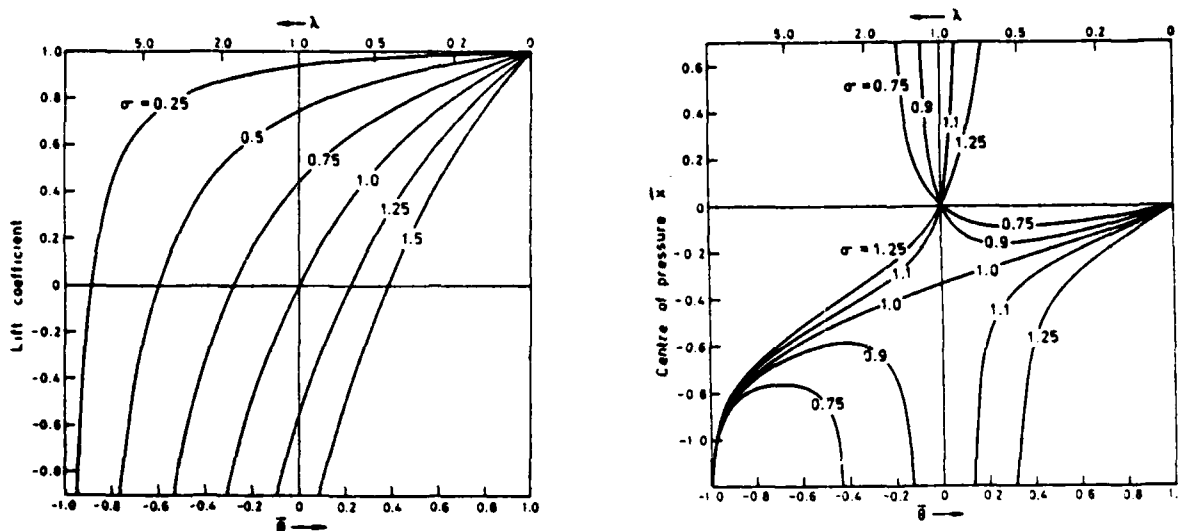


Figure 1-3. Lift and center of pressure for flat plates.

Finally, I want to mention some extensions of the ideas discussed here, namely to unsteady flows and wakes, and to non-rigid walls. Unsteadiness is of importance for determining development of flows from rest, for (dynamic) stability considerations, and for oscillatory flows. When one includes unsteadiness in the extreme-ground-effect theory, one must also concern oneself with the dynamics of the wake vortex sheet shed behind the airfoil as it moves. This sheet has non-zero strength only

for unsteady flow. The question (see Tuck, 1978) of whether such a non-trivial vortex sheet will or will not "roll up", is an interesting one that can be answered using the one-dimensional theory.

If the wall is not plane, but is still fixed and impermeable, the theory is unchanged, since  $h(x)$  still has the significance of the *net* clearance. However, an interesting generalisation is to the case of a *moveable* wall, in which there may be a second coupling between the pressure  $p$  in the air flow in the gap and the clearance  $h$ . This type of extended theory is discussed further in Chapter 5.

#### References for Chapter 1.

TUCK, E.O., "Unsteady small-gap ground effects", California Institute of Technology, *Engineering Science Report*, 78-1, 1978.

TUCK, E.O., "Steady flow and static stability of airfoils in extreme ground effect", *Journal of Engineering Mathematics*, 15 (1981) 89-102.

TUCK, E.O. and BENTWICH, M., "Sliding sheets: lubrication with comparable viscous and inertia forces", *Journal of Fluid Mechanics*, 135 (1983) 51-69.

TUCK, E.O. and NEWMAN, J.N., "Hydrodynamic interactions between ships", *10th Symposium on Naval Hydrodynamics*, Cambridge, Massachusetts, 1974. O.N.R.: Washington D.C.

WIDNALL, S.E. and BARROWS, T.M., "An analytic solution for two- and three- dimensional wings in ground effect", *Journal of Fluid Mechanics*, 41 (1970) 769-792.

## 2. Automobile Aerodynamics

It would be impossible to survey the field of automobile aerodynamics in one small chapter of this report, and I do not intend to attempt this. I shall concentrate on a few features relevant to the main theme, and hence on the influence of the ground plane. Recent background material is contained in the book by Sovran *et al* (1978).

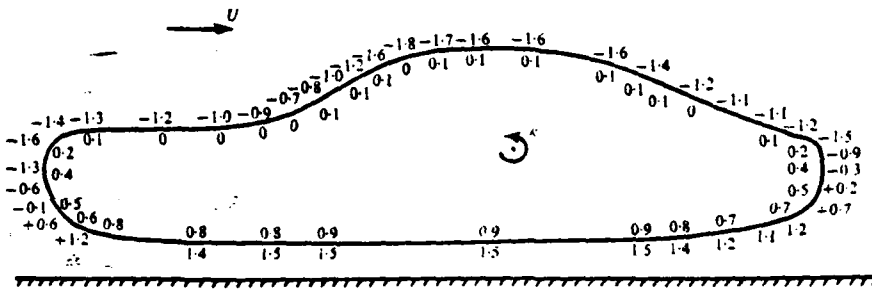


Figure 2-1. Flow about a Ford Capri.

Figure 2-1 is a suitable starting point for discussion. It shows the results of a two-dimensional irrotational flow computation (Tuck, 1971) on an automobile-like profile. In fact, this profile is that of the Ford Capri of that year. This figure has been reproduced by me and others (e.g. see a paper by Bearman, in Sovran *et al*, 1978) subsequently, and seems to have a lot to say about the general problem of automobile aerodynamics. That is a somewhat surprising conclusion at first thought, since the flow about a real automobile is neither two-dimensional nor irrotational.

Nevertheless, the computation makes those assumptions, and uses standard (cf. Hess and Smith, 1964) boundary-integral-equation methods to solve Laplace's equation exterior to an arbitrary profile, at an arbitrary distance from a plane boundary. In fact, two distinct boundary-value problems are solved. In the first ( $\phi_1$ ) there is assumed to be a uniform stream of unit magnitude at infinity, and there is no circulation about the profile; the figures written outside the profile are velocity magnitudes in that flow. The second flow ( $\phi_2$ ) has no uniform stream at infinity, but unit anti-clockwise circulation about the profile. The figures inside the profile are velocity magnitudes in that flow, which can be considered to have been generated by a fictitious unit vortex inside the profile.

The general solution is  $\phi = U\phi_1 + \kappa\phi_2$ , where  $U$  is the vehicle speed and  $\kappa$  the actual circulation about the profile. Unfortunately, we don't know the value of  $\kappa$  in advance, for an arbitrary bluff body. If the body is sufficiently airfoil-like, a Kutta-like condition can be used to determine  $\kappa$ , and we return to that case later.

In the meantime, what is the consequence of not knowing the value of  $\kappa$ ? Interestingly, there is *almost no* consequence, as far as the flow over the top of the vehicle is concerned, as can be noted from the relatively small inside figures over the top, relative to the outside figures. That is, the  $\kappa = 0$  solution is adequate to describe above-vehicle flows. It is tempting, and perhaps even correct, to extend this conclusion, and to claim validity for a zero-circulation three-dimensional irrotational-flow computation (in which the flow beneath the vehicle can be ignored), as a predictor of above-vehicle velocities and pressures. This is because the major defect of such a computation will be lack of treatment of the separated wake, but, insofar as the flow ahead of the wake is concerned, the wake serves mainly as a determinant of the circulation, and we have seen that circulation is of minor importance over the top of the vehicle.

In contrast, the circulation is of fundamental importance for the flow beneath the profile, as is evidenced from the relatively large inside numbers there. Thus wake conditions at the rear end are critical in determining under-vehicle flows, and, via the circulation, the net lift force on the vehicle. In three dimensions, induced drag will also be profoundly influenced by such matters; of course, in contrast to a wing, an automobile needs no lift, and hence induced drag can be eliminated if the section-wise circulation is zero. The pair of trailing vortices one often sees behind cars on a dusty road is a manifestation of this induced drag.

This point is illustrated further by noting that since  $\phi = U\phi_1 + \kappa\phi_2$  is a linear function of  $U$  and  $\kappa$ , then the lift  $F$  per unit span is necessarily a *quadratic* function of these two parameters, namely  $F = F_{11}U^2 + F_{12}U\kappa + F_{22}\kappa^2$ , where  $F_{11}, F_{12}, F_{22}$  can be computed by suitably integrating the numbers written on Figure 1. For the Ford Capri profile, it turns out that  $F_{11} = -0.10\rho L^2$ ,  $F_{12} = -1.27\rho$ ,  $F_{22} = -0.34\rho/L^2$ . Note that in the absence of ground effect, we should have necessarily  $F_{11} = F_{22} = 0$ , and  $F_{12} = -\rho$ , by the Kutta-Joukowski theorem. The term in  $F_{11}$  is present even in the absence of circulation, and would in the present case imply a small downward force, if one had designed the vehicle with  $\kappa = 0$  to eliminate induced drag.

The above discussion, while restricted to two dimensional or nearly two-dimensional flow, has been based on a computation that does not assume a thin body or a small gap. The qualitative conclusions become more accurate as the body becomes thin and the gap small, however. Nevertheless, so long as the body is bluff, the circulation  $\kappa$  remains unknown.

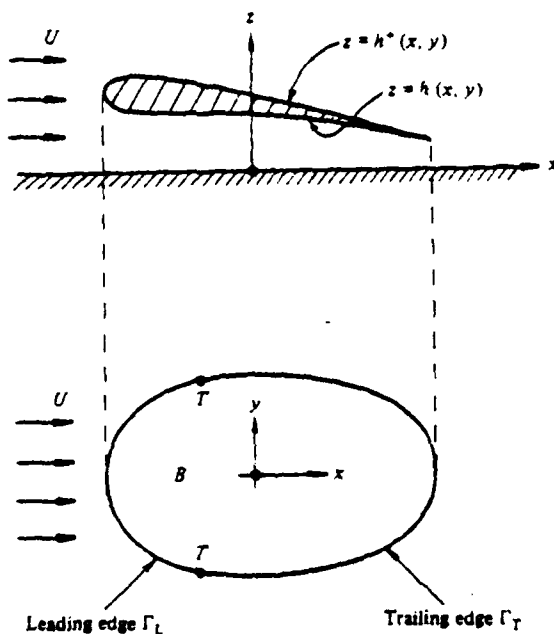


Figure 2.2. Co-ordinate sketch.

Let us now turn to the case of thin bodies in extreme ground effect (Tuck, 1983). This is the three-dimensional generalisation of Chapter 1, and is relevant to very streamlined and low-to-the-ground vehicles, eg. racing cars. Now we do have a means to determine the circulation  $\kappa$ , since a smooth-detachment or Kutta condition must apply at the trailing edge. The vehicle is assumed to have an outline curve (as seen from above) of the form  $\Gamma = \Gamma_L + \Gamma_T$ , with a transition point  $T$

between leading edge  $\Gamma_L$  and trailing edge  $\Gamma_T$ , as in Figure 2-2.

The mathematical problem for the flow beneath the vehicle is to find a velocity potential  $\phi(x, y)$  satisfying

$$\frac{\partial}{\partial x} \left( h \frac{\partial \phi}{\partial x} \right) + \frac{\partial}{\partial y} \left( h \frac{\partial \phi}{\partial y} \right) = 0 \quad (2.1)$$

inside  $\Gamma$ , subject to

$$\phi = Ux \quad (2.1)$$

on  $\Gamma_L$ , and

$$\phi_x^2 + \phi_y^2 = U^2 \quad (2.3)$$

on  $\Gamma_T$ . The justification for these equations can be found in Tuck (1983) and Tuck (1980). In fact, equation (2.1) is just the usual shallow-water equation for a steady flow with negligible vertical velocity in a region of non-constant "depth"  $h(x, y)$ , equation (2.2) matches that flow to the incident stream at the leading edge, and equation (2.3) is the Kutta condition matching to the ambient pressure at the trailing edge.

A difficulty is that the transition point  $T$  is not known in advance. That is, we'd better be clear what we actually mean by a "leading" or a "trailing" edge. It seems to me that this question has received insufficient attention from aerodynamicists. However, that is excusable, since in open-air linearised lifting-surface theory,  $T$  is necessarily located at the extremities of the wing, ie. the leading edge always changes into a trailing edge at the *wing tips*. I believe that this is true in all linearised flows, but fails in the present case because the problem is non-linear, in the sense that  $\phi$  is not everywhere close to  $Ux$ .

Clearly, a leading edge is one where fluid passes from *outside* the contour of the wing to *inside* it, and *vice versa* for a trailing edge. However, this doesn't quite settle it, since there are two insides, namely *inside above* and *inside below*. Let us then (at least in the purely geometric sense) be quite specific. We define the mean horizontal-plane velocity vector  $\bar{q}$  on  $\Gamma$  to be the average of the vector horizontal fluid velocities above and below the wing there. Then this part of  $\Gamma$  belongs to  $\Gamma_L$  if  $\bar{q} \cdot \mathbf{n} < 0$  and to  $\Gamma_T$  if  $\bar{q} \cdot \mathbf{n} > 0$ , where  $\mathbf{n}$  is the unit outward normal to  $\Gamma$  in the horizontal plane.

In classical open-air linearised aerodynamics,  $\bar{q} = Ui$ , since the perturbation velocities above and below the lifting surface are equal and opposite. Hence the transition point  $T$  between leading and trailing edge must occur where the contour  $\Gamma$  is locally parallel to the free stream, ie. at an extremity. The same applies even in ground effect, if we linearise the problem in the manner of Widnall and Barrows (1970).

However, in the fully-non-linear problem, this is not necessarily the case. Note that in extreme ground effect, the flow beneath the vehicle is governed by (2.1)-(2.3), but the flow *above* it is (to leading order) just the undisturbed stream  $\phi = Ux$ . Hence, in carrying out the averaging process to find  $\bar{q}$ , we use  $Ui$  for the above-vehicle component, but  $\nabla\phi$  for the under-vehicle component, and since  $\phi$  is not a small perturbation of  $Ux$ , we no longer get  $\bar{q} = Ui$ . In fact (cf. Tuck 1983, Newman 1982), the local streamline at  $T$  necessarily makes an angle with the  $x$ -axis that is twice the angle  $\pi/2$  by  $\Gamma$ .

In any case, it is not difficult to build determination of the location of  $T$  into any computational procedure for solving the boundary-value problem (2.1)-(2.3). Since the problem is non-linear (because of (2.3)), we shall be forced to use an iterative procedure, and we can simply adjust the location of  $T$  at each iteration step, so that  $\bar{q} \cdot \mathbf{n} = 0$  at  $T$ . Figures 2-3 and 2-4 show sample computations from Tuck (1983) for a circular lifting surface, at positive and negative angle of attack, respectively. These computations were done with a special (exponential) variation in clearance, such that (2.1) possesses a (modified Bessel function) family of eigensolutions, which can be

used to simplify the task. Work is proceeding on a direct attack on the problem for more-realistic contours and clearances.

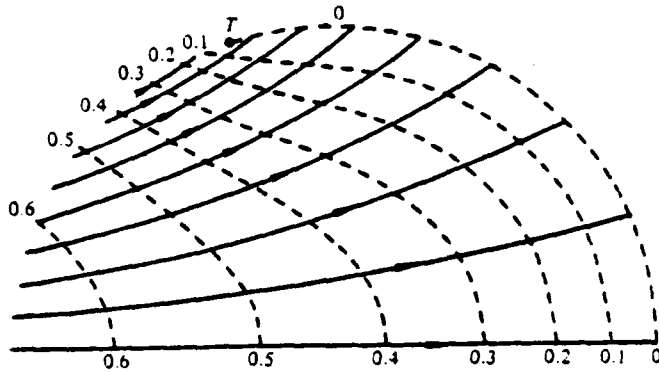


Figure 2-3. Circular wing at positive angle of attack.

Meanwhile, Figures 2-3 and 2-4 at least illustrate some important phenomena in three-dimensional extreme ground effect. Figure 2-3 (*positive* angle of attack) has positive pressure and lift, and shows fluid being deflected outward by this positive pressure, while the transition point T is moved forward of the lateral extremity of the circle. Conversely, Figure 2-4 (*negative* angle of attack) has negative pressure (except for a region of very small positive pressure near the rear) which sucks fluid in from the side, and the transition point T is aft of the lateral extremity.

Some recent racing car designs have exploited the ground effect for negative lift, and a feature of these designs is the use of "skirts" or lateral barriers near the extremities to prevent the inward flow.

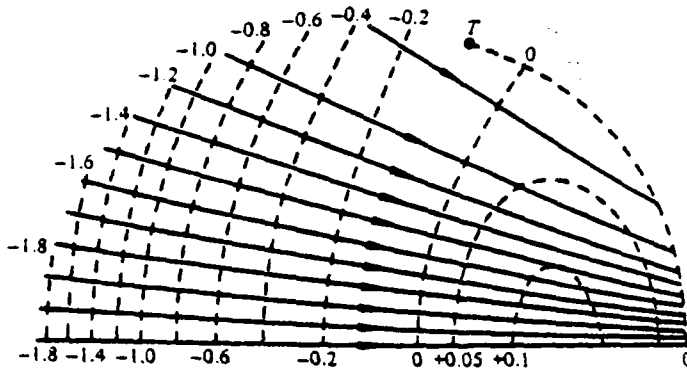


Figure 2-4. Circular wing at negative angle of attack.

**References for Chapter 2.**

HESS, J.L. and SMITH, A.M.O., "Calculation of non-lifting potential flow about arbitrary three-dimensional bodies", *Journal of Ship Research*, 8 (1964) 22-44.

NEWMAN, J.N., "Analysis of small-aspect-ratio lifting surfaces in ground effect", *Journal of Fluid Mechanics*, 117 (1982) 305-314.

SOVRAN, G., MOREL, T., and MASON, W.T., *Aerodynamic Drag Mechanisms of Bluff Bodies and Road Vehicles*, Plenum Press, 1978.

TUCK, E.O., "A non-linear unsteady one-dimensional theory for wings in extreme ground effect", *Journal of Fluid Mechanics*, 98 (1980) 33-47.

TUCK, E.O., "Non-linear extreme ground effect on thin wings of arbitrary aspect ratio", *Journal of Fluid Mechanics*, 136 (1983) 73-84.

WIDNALL, S.E. and BARROWS, T.M., "An analytic solution for two- and three- dimensional wings in ground effect", *Journal of Fluid Mechanics*, 41 (1970) 769-792.

### 3. Shallow-Water Waves at Discontinuities

Shallow-water waves represent perhaps the prototype small-gap flow, the water depth being the "small gap". The water is shallow if  $h$  is small compared with all horizontal scales of interest, of which perhaps the most important is the wavelength  $\lambda$ . For that reason, shallow-water theory is sometimes referred to as "long-wave" theory, a terminology that I have long opposed, as placing emphasis on too-narrow an interpretation of the shallowness property.

In the present lecture, I shall only discuss linear shallow-water waves, described by the wave equation

$$\frac{\partial h}{\partial t} + \frac{\partial}{\partial x} \left( h \frac{\partial \phi}{\partial x} \right) + \frac{\partial}{\partial y} \left( h \frac{\partial \phi}{\partial y} \right) = \frac{1}{g} \frac{\partial^2 \phi}{\partial t^2} \quad (3.1)$$

where the depth  $h = h(x, y, t)$  in general can depend on both horizontal space co-ordinates and time, and  $\phi = \phi(x, y, t)$  is a horizontal velocity potential. One can interpret  $\phi(x, y, t)$  as a *depth-averaged* three-dimensional velocity potential, or as the value of such a potential at the bottom, or at the free surface, etc. Although some authors make a big deal of this sort of distinction, it is really rather irrelevant, the point being that, consistent with the shallowness assumption,  $\phi$  depends only weakly on the vertical co-ordinate  $z$ . Note that the actual linearised wave elevation is  $-\phi_t/g$ .

The bottom-motion term  $\partial h/\partial t$  is not often included in (3.1). However, an important application where it is of crucial importance is for the study of generation of tsunamis by earthquakes, with  $h(x, y, t)$  as the given(?) ground displacement due to the earthquake. Of course, as a practical matter,  $h(x, y, t)$  is known only sketchily at best. In any case, I have made a plea (Tuck 1979) that (3.1) be taken seriously as the governing equation for tsunami generation, propagation, and reception. Effects of dispersion and non-linearity are of very little significance for much of the history of these extremely long and low-amplitude waves.

Notice that if there is no time dependence, (3.1) is just the same equation as used in Chapter 2 to describe under-vehicle air flows. The famous derivation by Friedrichs (1948) makes it clear why a similar equation will always hold for irrotational incompressible flows in a small gap. Although, with or without time dependence, (3.1) is not entirely straightforward to solve, analytically or numerically (see again Tuck 1979, for warnings about numerical artifacts), it is at least a conventional wave equation, and there are few mysteries once we accept its validity.

However, one often wishes to use it where it is not formally valid, ie. where there are horizontal length scales comparable to  $h$ . In particular, it is not entirely obvious what are the correct *boundary conditions* in some cases, especially where the boundaries are not vertical. Stoker (1957, p.420) gives some guidance, but never addresses the difficulty that (3.1) seems to lose its validity near the boundary.

Perhaps the simplest example where this difficulty arises is Lamb's (1932, p.262) treatment of reflection and transmission by a step change in depth. Suppose

$$h = \begin{cases} h_-, & x < 0 \\ h_+, & x > 0 \end{cases}$$

and

$$\phi = \begin{cases} e^{ik_-x - i\sigma t} + \rho e^{-ik_-x - i\sigma t}, & x < 0, \\ \tau e^{ik_+x - i\sigma t}, & x > 0, \end{cases}$$

where

$$gh_{\pm}k_{\pm}^2 = \sigma^2$$

Physically, this corresponds to a unit-amplitude wave in  $x < 0$ , being reflected (co-efficient  $\rho$ ) and transmitted (co-efficient  $\tau$ ) into  $x > 0$ . Equation (3.1) is satisfied for all values of  $\rho$  and  $\tau$ , and our task is to match the two parts of the solution across  $x = 0$  to find  $\rho$  and  $\tau$ .

Lamb uses continuity of  $\phi$  and of  $h\phi_x$ , namely

$$1 + \rho = \tau$$

and

$$h_- k_- (1 - \rho) = h_+ k_+ \tau$$

to establish

$$\rho = \frac{1 - \mu^{\frac{1}{2}}}{1 + \mu^{\frac{1}{2}}}$$

and

$$\tau = \frac{2}{1 + \mu^{\frac{1}{2}}}$$

where  $\mu = h_+/h_-$  is the depth ratio. The Lamb continuity conditions are similar to those of Stoker. Physically, continuity of  $\phi$  implies continuity of wave elevation, and continuity of  $h\phi_x$  implies continuity of mass, so these conditions appear rather natural and correct.

However, continuity of  $h\phi_x$ , while  $h$  itself jumps, implies that  $\phi_x$  jumps; ie. there is a step discontinuity in the horizontal velocity, which seems neither natural nor correct at first sight. In fact we saw this difficulty already in Chapter 1, and it is characteristic of situations where the small-gap assumption breaks down locally. Here the breakdown is very acute, since the length scale for horizontal changes is not only not large compared to  $h$ , but actually vanishes at  $x = 0$ .

The resolution of this paradox is not difficult to achieve by matching. That is, we abandon (3.1) near  $x = 0$ , and seek instead a solution of the full equations of motion, which means in the present case the two-dimensional Laplace equation (there being no  $y$ -dependence) in the vertical plane, namely

$$\phi_{xx} + \phi_{zz} = 0$$

for  $x = O(h)$ ,  $z = O(h)$ . But, in such a spatially-stretched region, the free surface appears locally rigid (ie.  $\phi_z = 0$  on  $z = 0$ ) a conclusion that can be derived formally from the exact free-surface condition, for waves with  $\lambda \gg h$ , ie. wavelengths far in excess of the length scales of interest locally. The local problem is thus a simple streaming flow through a rigid-walled channel, of step-changing cross-section, as in Figure 3-1, and can be solved easily, eg. by conformal mapping. In fact, this qualitative picture applies for a general depth change, not necessarily restricted to a sudden jump, but in the general case the numerical solution may not be so easy.

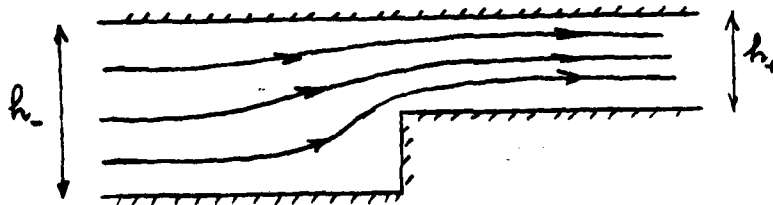


Figure 3-1. Sketch of local flow near depth change.

The result (see Tuck 1976) is that we confirm Lamb's jump conditions, and in addition obtain a first correction to the  $\phi$ -continuity condition, namely that there is a (small,  $O(h)$ ) jump in the value of  $\phi$  across  $x = 0$ , of magnitude

$$\Delta\phi = 2C.h\phi_x$$

(recalling that  $h\phi_x$  is continuous), where  $C$  is a uniquely-determined co-efficient depending on the detailed shape of the depth change. For the specific case of a step as in Figure 3-1, we have

$$2\pi C = \frac{\mu^2 + 1}{\mu} \log \left| \frac{\mu + 1}{\mu - 1} \right| - 2 \log \left| \frac{4\mu}{\mu^2 - 1} \right|$$

The effect on the Lamb problem is that the reflection co-efficient is corrected to

$$\rho = \frac{1 - \mu^{\frac{1}{2}}}{1 + \mu^{\frac{1}{2}}} \left[ 1 - 4iC \frac{\mu^{\frac{1}{2}}}{1 - \mu} k_+ h_+ + O(h^2) \right]$$

Note that, (for  $\mu \neq 1$ ), the new  $O(h)$  term affects only the *phase* of the reflection co-efficient; the first correction to its *amplitude* arrives only at the next  $O(h^2)$  correction. Similar but less general results were obtained by Bartholomeuss (1958).

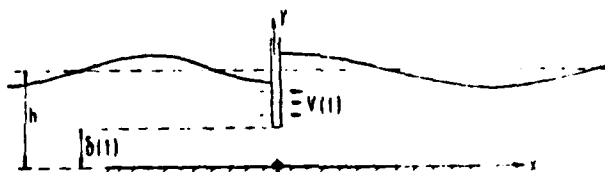


Figure 3-2. Sketch of flow for paddle wavemaker.

The ideas behind the above matching can be generalised in a number of other shallow-water problems. For example, in my own work, I have studied paddle-type wave-makers (Tuck 1974) that do not occupy the whole water depth, thereby leaving a bottom gap as they oscillate. As in the Lamb problem, one can match a solution of (3.1) (in this case, a purely out-going wave) to a local rigid-free-surface flow near the paddle, as in Figure 3.2. This leads to predictions of the loss in efficiency of the paddle, as a function of the gap size. If the gap size varies with time during the stroke, as for example it would if the paddle were swinging like a pendulum, the corollary is a distorted wave form, in spite of the basic linearity of the problem.

As part of a general study of water-wave (not necessarily shallow) transmission through small holes in vertical barriers, the shallow-water special case was treated in an Appendix to Guiney *et al* (1972) by similar methods. The transmission co-efficient that results can be written

$$\tau = 1/(1 + ikC)$$

where  $k = 2\pi/\lambda$  is the wave number, and

$$C = -\frac{D}{\pi} \log \left( \pi \frac{a}{D} \sin \frac{\pi h}{D} \right)$$

in the local geometry of Figure 3-3.

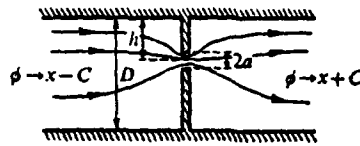


Figure 3-3. Local flow through a hole in a wall.

A recent study (Tuck 1980) of waves incident upon a basin partially protected by a reef as in Figure 3-4, used similar concepts. The results for the natural frequencies of the basin as a function of gap size compared well with model tests (Tuck *et al*, 1980).

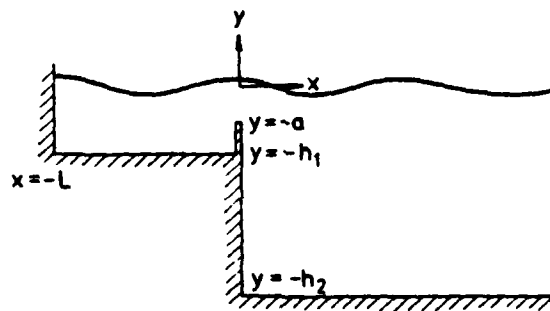


Figure 3-4. Flow geometry for submerged reef.

Finally, I should point out that a slender ship moving in shallow water provides a good example of an apparent discontinuity in application of (3.1) (or its equivalent for some steady flows). Again, one has to match with a local flow near each cross-section of the ship, in which the free surface is replaced by a rigid wall. Such problems are discussed in Tuck 1976 and 1978; see also Yeung and Tan 1980.

### References for Chapter 3

BARTHOLOMEUSZ, E.F., "The reflection of long waves at a step," *Proceedings of the Cambridge Philosophical Society*, 54 (1958) 106-118.

FRIEDRICHS, K.O., "On the derivation of the shallow-water theory," *Communications on Pure and Applied Mathematics*, 1 (1948) 81-85.

GUINEY, D.C., NOYE, B.J., and TUCK, E.O., "Transmission of water waves through small apertures," *Journal of Fluid Mechanics*, 55 (1972) 149-161.

LAMB, H., "Hydrodynamics" (6th edn.) (1932), Cambridge and Dover Publications.

STOKER, J.J., "Water Waves" 1957, New York : Interscience.

TUCK, E.O., "Paddle-type wave-makers in shallow water," *International Symposium on the Dynamics of Marine Vehicles and Structures in Waves*, 1974, Proceedings, University College, London.

TUCK, E.O., "Some classical water-wave problems in varying depth", *Symposium on Waves in Water of Varying Depth* 1976, Proceedings (ed. Provis, D.G. and Radok, J.R.M.), Berlin : Springer-Verlag.

TUCK, E.O., "Hydrodynamic problems of ships in restricted waters", *Annual Reviews of Fluid Mechanics*, 10 (1978) 33-44.

TUCK, E.O., "Models for predicting tsunami propagation", *N.S.F. Workshop on Tsunamis*, 1979, Proceedings, Tetra Tech Inc., Pasadena, California.

TUCK, E.O. "The effect of a submerged barrier on the natural frequencies and radiation damping of a shallow basin connected to open water", *Journal of the Australian Mathematical Society, Series B*, 22 (1980) 104-128.

TUCK, E.O., ALLISON, H., FIELD, S., and SMITH, J., "Effects of a submerged reef chain on sea-level oscillations in Western Australia", *Australian Journal of Marine and Freshwater Research*, 31 (1980) 719-727.

YEUNG, R.W. and TAN, W.T., "Hydrodynamic interactions of ships with fixed obstacles", *Journal of Ship Research*, 24 (1980) 50-59.

#### 4. Sliding Sheets

G. I. Taylor's famous movie (1967) on low Reynolds' number fluid dynamics contains an entertaining demonstration of paper sheets sliding easily over a smooth table top, an experiment repeatable by anyone. Taylor described this phenomenon as an example of fluid lubrication, which it certainly is. What is far from obvious is that the *viscosity* of the fluid plays any role. That is, could the paper be "flying", like an airfoil in ground effect?

I used this example often when I first worked in this area, and was originally quite confident that the answer to the above question is "Yes". If so, the inviscid analysis (*e.g.* from Chapter 1, for a sheet of large aspect or width/length ratio) predicts that if  $h(x)$ ,  $0 < x < L$ , is the clearance, then the pressure under the sheet is given by

$$p = p_{\infty} + \frac{1}{2} \rho U^2 [1 - h(L)^2/h(x)^2] \quad (4.1)$$

from which we can obtain the lift  $F$  and moment  $M$  per unit width. However, there are two difficulties:

- (i)  $F < \frac{1}{2} \rho U^2 L$ , *i.e.* there is an upper limit on the weight of sheets that can fly.
- (ii)  $M \neq 0$  about the centre, *i.e.*, a uniform sheet cannot be in pitching equilibrium.

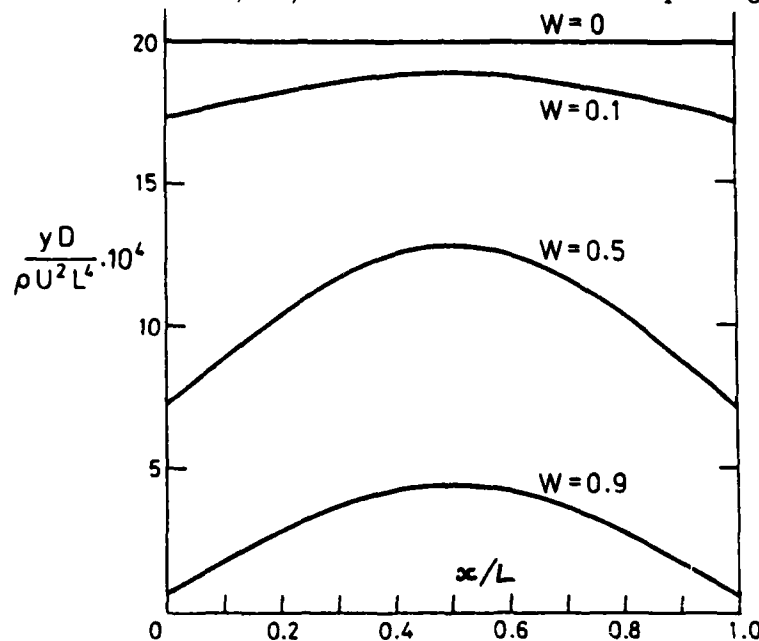


Figure 4-1. Flexible sheets, highest-flying bending modes.

The latter is a major difficulty, and I attempted to resolve it within the inviscid theory by allowing the sheet to *bend* (Tuck, 1982). The resulting analysis is an interesting exercise in non-linear coupled aerodynamics and elasticity, and an infinite number of equilibrium configurations was obtained. Figure 4-1 shows the first (highest-flying) mode, for various weights. The scale of the figure is inversely proportional to the stiffness  $D$ , and hence this theory predicts that a nearly-rigid sheet must fly very close to the ground.

However, air is viscous, and in particular, the Reynolds' number based on the gap clearance  $h$  is not necessarily large. If viscosity  $\mu$  is dominant, we might expect a fully-developed Couette-type

flow, with a nearly-linear velocity profile across the gap, modulated by corrections that vary slowly along the gap. This is typical of "lubrication theory", and leads (for a flat plate at angle of attack  $\alpha$ ) to a pressure distribution given by

$$p = p_\infty + \frac{3\mu\alpha x(L-x)}{h(\frac{1}{2}L)h(x)^2} \quad (4.2)$$

This result is only true for sufficiently small Reynolds' number, in contrast to (4.1), which is only true for sufficiently large Reynolds' numbers. Equation (4.2) also has a defect like (ii) above, in that the moment about the center point is non-zero — indeed the sign is opposite to that predicted by equation (4.1).

So what actually happens to a non-flexible uniform sheet? It cannot be in pitching equilibrium at either high or low Reynolds' number. Fortunately, the sign variation in moment at these extremes suggests that there will exist an intermediate Reynolds' number where the moment about the center is zero. I now give a brief summary of a study of this problem by Tuck and Bentwich (1983).

The Reynolds' number of interest is actually a special one, namely

$$R = \frac{Uh(0)^2}{\nu L} \quad (4.3)$$

which is a small multiple  $h(0)/L$  of the Reynolds' number based upon clearance  $h$ , and an even smaller multiple  $(h(0)/L)^2$  of that based on sheet length  $L$ . Hence if  $R = O(1)$ , both the latter Reynolds' numbers are large, and an inviscid theory applies in all regions of flow except the main gap. In particular, the entrance-region flow is inviscid, and in fact is the same as Figure 1-2.

But we are mainly interested in what is happening in the main gap region, and it is not hard to show by asymptotic stretching that the appropriate equation is the boundary-layer equation

$$\psi_y \psi_{xy} - \psi_x \psi_{yy} = -\frac{1}{\rho} p'(x) + \nu \psi_{yyy} \quad (4.4)$$

for the stream function  $\psi(x, y)$ . We have to solve equation (4.4) subject to no-slip boundary conditions on both walls; this gives four conditions for a 3rd-order equation, enabling simultaneous determination of the (unknown) pressure  $p(x)$ .

Before we can start solving (4.4) we need "initial" conditions at the starting station  $x = 0$ , and "exit" conditions at the station  $x = L$  where the gap flow merges with the inviscid outer flow above the sheet. The former is a requirement that the flow match an entrance flow as in Figure 1-2, with an arbitrary velocity  $u(0)$  at  $x = \infty, 0 < y < h(0)$ , i.e., the entrance profile is a uniform stream of to-be-determined magnitude. How is  $u(0)$  determined? The pressure  $p(x)$  must commence with the Bernoulli value

$$p(0) = p_\infty + \frac{1}{2}\rho U^2 - \frac{1}{2}\rho u(0)^2 \quad (4.5)$$

at  $x = 0$ , and end with the free-stream value

$$p(L) = p_\infty \quad (4.6)$$

at  $x = L$ . Equation (4.6) is the "exit" condition that finally fixes  $u(0)$ .

We now have enough conditions to solve (4.4). The resulting boundary-value problem is an "inverse" problem, in the terminology of Keller (1978), since  $p(x)$  is not prescribed as it is in the more usual external or "direct" boundary-layer problems. However, there are many practical numerical methods available, and we can consider this problem as easily solveable.

Figure 4-2 shows a typical set of streamlines for a case with  $h(0)/h(L) = 4$  with a very tight constriction. In fact whenever this "contraction ratio" exceeds 2, there is a separated "bubble" attached to the upper (sloping) face, within which there is reversed flow. Nevertheless, the computation proceeds without difficulty.

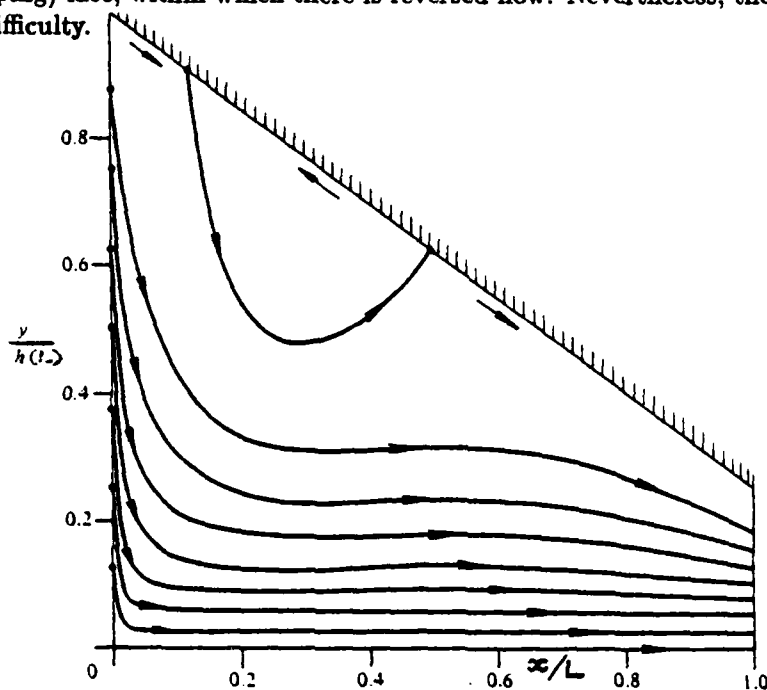


Figure 4-2. Streamlines at  $R = 9.6$ ,  $\bar{\alpha} = 0.75$ .

Figure 4-3 displays the main pressure results for the flow of Figure 4-2. These figures show the inviscid (4.1) and lubrication (4.2) approximations, together with a useful "linearised" approximation described in detail in Tuck and Bentwich (1983). The curves labelled "exact" are numerical boundary-layer computations to high precision.

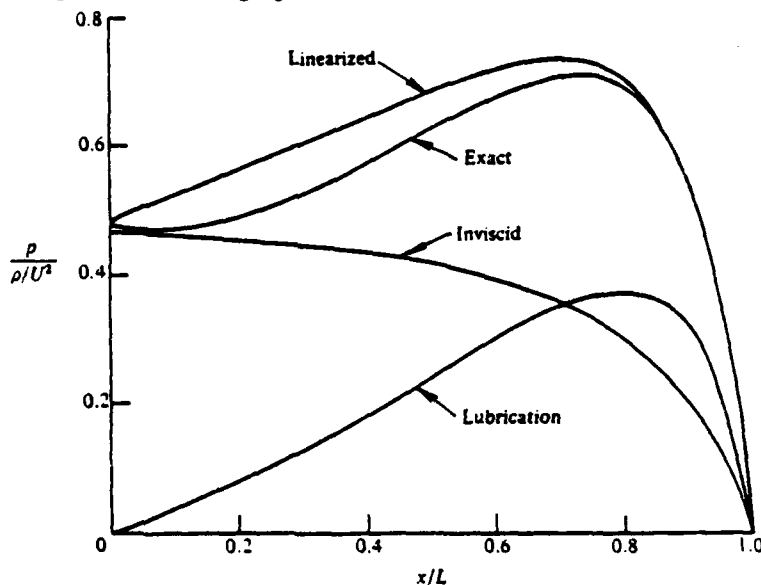


Figure 4-3. Pressure results, flow of Fig.4-2.

Figure 4-4 is a final result, obtained by integrating this pressure, for those cases where the centre of pressure is at mid-chord. This figure gives the "design charts" for steady flight of uniform sheets in pitching equilibrium.

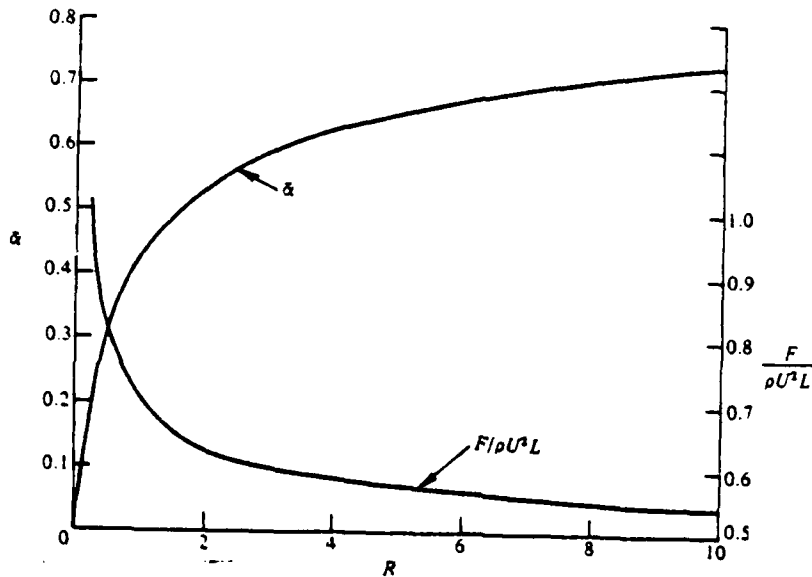


Figure 4-4. Lift and angle of attack for uniform sheets.

#### References for Chapter 4

KELLER, H.B. "Numerical methods in boundary-layer theory", *Annual Reviews of Fluid Mechanics*, 10 (1978) 417-433.

TAYLOR, Sir Geoffrey, "Low-Reynolds-number flows", *Encyclopaedia Britannica Educational Corporation* (16mm. color sound film) 1967.

TUCK, E.O., "An inviscid theory for sliding flexible sheets," *Journal of the Australian Mathematical Society, Series B*, 23 (1982) 403-415.

TUCK, E.O. and BENTWICH, M., "Sliding sheets: lubrication with comparable viscous and inertia forces", *Journal of Fluid Mechanics*, 135 (1983) 51-69.

## 5. Wings Over Water

Suppose we have an extreme ground-effect air flow about a thin airfoil like that of Figure 5-1. In contrast to the flows treated in previous chapters, the *ground plane* is neither a ground nor a plane. Instead, it is supposed to be a free water surface, whose main property is **deformability** in response to aerodynamic pressure. We assume now that  $h(x)$  denotes the height of the under-surface of the airfoil relative to the undisturbed water surface, and  $\eta(x)$  is the elevation of the disturbed water surface.

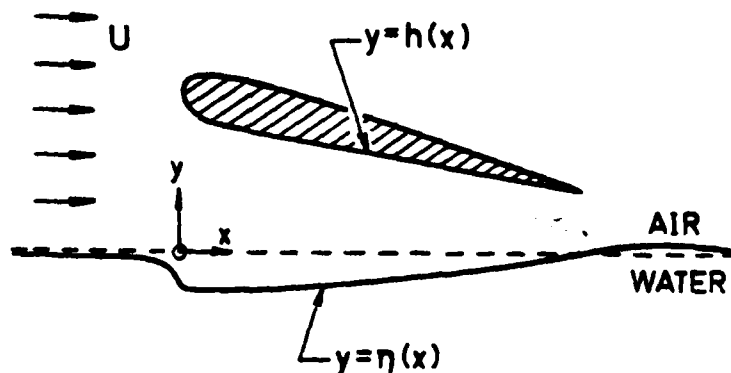


Figure 5-1. Sketch of airfoil near water.

A one-dimensional air flow is assumed to occur in the small-gap region, and hence the pressure distribution varies like the negative inverse square of the local clearance, namely as

$$p(x) = p_{\infty} + \frac{1}{2} \rho_A U^2 \left[ 1 - \left( \frac{h(L) - \eta(L)}{h(x) - \eta(x)} \right)^2 \right] \quad (5.1)$$

where  $p_{\infty}$  is the ambient or atmospheric pressure at infinity, and  $\rho_A$  is the density of the (incompressible) air.

We need one more equation relating  $p(x)$  and  $\eta(x)$ . First let us assume (Tuck 1984) that this equation is

$$p(x) = p_{\infty} - \rho_W g \eta(x), \quad (5.2)$$

i.e. the pressure is **hydrostatic**, with  $g$  as the acceleration of gravity and  $\rho_W$  as water density. In effect, we are assuming that the water does not move at all, but its surface merely deforms statically in response to the aerodynamic pressure. Some direct justification of this type of assumption is provided in Tuck (1975).

Before looking at the consequence of (5.2), it is instructive to note that the relationship (5.2) is a simple linear representation of potential energy storage by the deformable surface  $y = \eta(x)$ , and, as such, could be achieved in other ways. For example, suppose the "water" were replaced by a type of elastic medium, known in the theory of foundations as a "Winkler soil" (Selvadurai 1970), consisting of a distribution of independent linear springs. Then, again, there would be a linear pressure-versus-displacement relationship like (5.2), with a "*modulus of sub-grade reaction*" or spring constant per unit area, of magnitude  $\rho_W g$ . A qualitatively similar result also holds if we allow the air to be compressible, even if the ground is still rigid and plane, since again we should be providing potential energy storage.

In any case, if we accept (5.2) and combine it with (5.1), we can eliminate  $\eta(x)$ , obtaining a single non-linear algebraic equation for the pressure  $p(x)$ , namely

$$h(x) - [h(L) - \eta(L)](1 - P(x))^{-\frac{1}{2}} = -\frac{1}{2} \frac{\rho_A}{\rho_W} \frac{U^2}{g} P(x), \quad (5.3)$$

where

$$P(x) = \frac{p(x) - p_\infty}{\frac{1}{2} \rho_A U^2}. \quad (5.4)$$

Equation (5.3) can be re-written as a cubic polynomial equation for  $P(x)$ , and solved easily for any given  $h(x)$ . There are special significances to be attached to the parameter choices at which the *discriminant* of this cubic vanishes, i.e. where the number of real roots of (5.3) changes from one to three, and this is discussed further in Tuck, 1984. In particular, physically-acceptable solutions exist if  $h(x) > h(L)$  whenever  $x < L$ , i.e. the trailing edge is lower than any other point, while at the same time  $F < 1$ , where

$$F^2 = \frac{U^2}{gh(L)} \frac{\rho_A}{\rho_W}. \quad (5.5)$$

The parameter  $F$  is a kind of modified clearance-based Froude number, and the above requirement states that "sub-critical" flows exist at positive angle of attack. Figure 5-2 shows the computed free surface shape  $\eta(x)$  for a flat plate in some such cases.

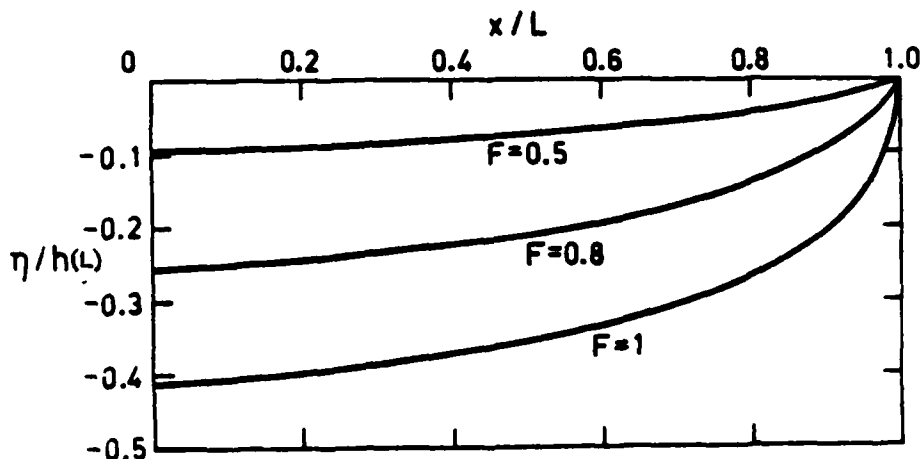


Figure 5-2. Hydrostatic free surface under flat plate.

In more recent work (Grundy and Tuck, 1984), the hydrostatic law (5.2) has been replaced by a true hydrodynamic model of the water surface. The simplest way to achieve this is to note that the right-hand side of (5.3) is just the water surface elevation  $\eta(x)$ ; if (5.2) does not hold, but instead we allow hydrodynamic effects, we simply replace the current right-hand side of (5.3) by the known  $\eta(x)$  produced by a given pressure distribution  $p(x)$ .

Since the hydrodynamic disturbance is small, because the free-surface slope  $\eta'(x)$  is everywhere small, the free-surface boundary condition can be linearised (for the flow in the water, if not in the air), and the solution of the hydrodynamic problem is as given for example in Wehausen and Laitone (1960; see also Tuck 1982). Thus (5.3) becomes

$$h(x) - [h(L) - \eta(L)](1 - P(x))^{-\frac{1}{2}} = \frac{1}{2} \frac{\rho_A}{\rho_W} \int_0^L P(\xi) K' \left( \frac{g}{U^2} (x - \xi) \right) d\xi, \quad (5.6)$$

where

$$K'(x) = -f'(x)/\pi - 2 \sin x H(x) \quad (5.7)$$

with  $f'(x)$  as an (even) auxiliary function for the sine and cosine integrals, and  $H$  the Heaviside step function. The problem is now reduced to a non-linear integral equation for  $P(x)$ .

An interesting paradox presents itself. We might hope (even *expect*?) that (5.6) reduces to (5.3) as  $U \rightarrow 0$ , i.e. as hydrodynamic effect become weaker. This almost happens! If we let the length-based Froude number  $F_L = U(gL)^{-1/2}$  tend to zero in (5.6), the right-hand side tends to that of (5.3), but **only** if both  $P(0)$  and  $P(L)$  also tend to zero in that limit. That is, the pressure distribution must return to atmospheric at both ends.

In fact, in solving (5.6) for general non-zero  $F_L$ , we can and do demand already that  $P(L) = 0$ , i.e. we enforce a Kutta condition that the pressure return to atmospheric at the trailing end. This is a freedom available to us since the end clearance  $h(L) - \eta(L)$  that appears explicitly in (5.6) is an extra unknown, and in practice we allow its value to vary until  $P(L) = 0$ . However, we have no reason to expect that  $P(0) = 0$  at any  $F_L$ , and in particular there appears no numerical evidence that (in general)  $P(0) \rightarrow 0$  as  $F_L \rightarrow 0$ . Hence it must be exceptional for solutions of (5.6) to approach solutions of (5.3) as  $F_L \rightarrow 0$ .

In any case, efforts are underway to solve (5.6) numerically. I show here (Figure 5-3) perhaps the most interesting of the preliminary outputs. These results are for a flat plate at various positive angles of attack in sub-critical flow at  $F \approx 0.7$ , as measured by (5.5). Hence the hydrostatic theory gives results like those of Figure 5-2, which have the property that  $P(0) \neq 0$ . Figure 5-3 now gives computed values of  $P(0)$  as a function of  $F_L$ , at fixed  $F$ . There is no tendency for  $P(0)$  to vanish as  $F_L \rightarrow 0$ , nor in fact for  $P(x)$  as computed by this program to approach that computed from the hydrostatic theory, at any  $x$ .

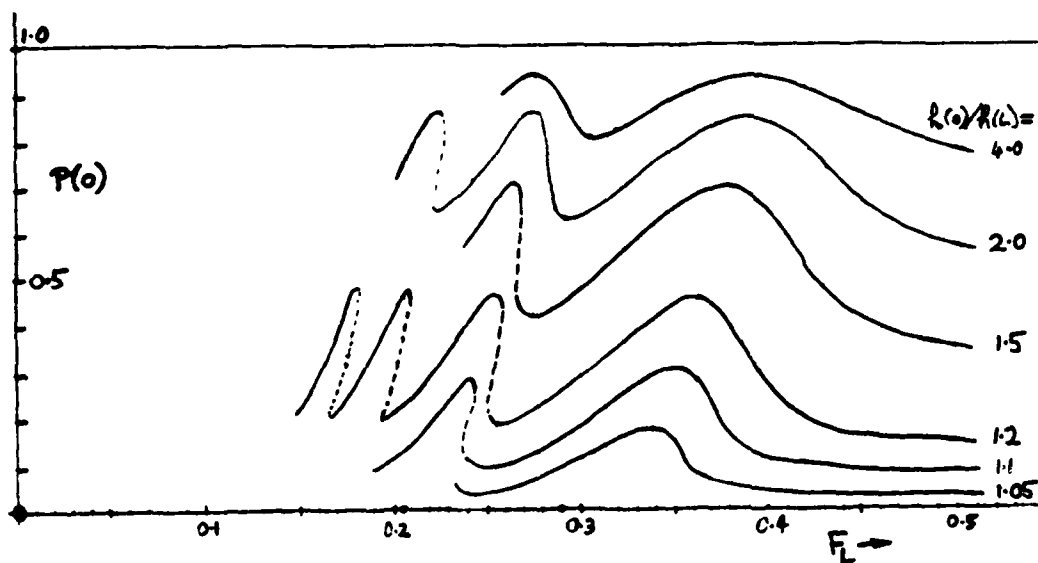


Figure 5-3. Leading-edge pressure on a flat plate.

Another remarkable feature of the finite- $F_L$  results, displayed in Figure 5-3, is that they are non-unique in some parameter ranges! For example, at about  $F_L = 0.25$ , a vertical line intersects the curve labelled  $h(0)/h(L) = 1.2$  in three places. I must confess that we are presently only able to compute two of these three solutions, the dashed portion of the curve being inferred. There are obviously a number of things happening here that are not easy to understand!

On a more positive closing note, Figure 5-4 shows some results that do approach the hydrostatic theory as  $F_L \rightarrow 0$ . These are for a (parabolic) curved airfoil, which is fore-and-aft symmetric. In such a case, the hydrostatic theory demands a fore-and-aft symmetric pressure distribution. Thus, if  $P(L) = 0$ , necessarily  $P(0) = 0$  also, at  $F_L = 0$ . The numerical work for finite  $F_L$  confirms this; although there is no fore-and-aft symmetry of  $P(x)$  so long as  $F_L \neq 0$ , such symmetry is approached as  $F_L \rightarrow 0$ , and, better yet, the hydrostatic results are approached in that limit for all  $x$ . Note of course that this limit is still a somewhat singular one, since the flow at any  $F_L \neq 0$  contains waves, and these waves become shorter and shorter as  $F_L \rightarrow 0$ , even though (in the present case of a fore-and-aft symmetric curved body, if not for a flat plate) their amplitude is tending to zero.

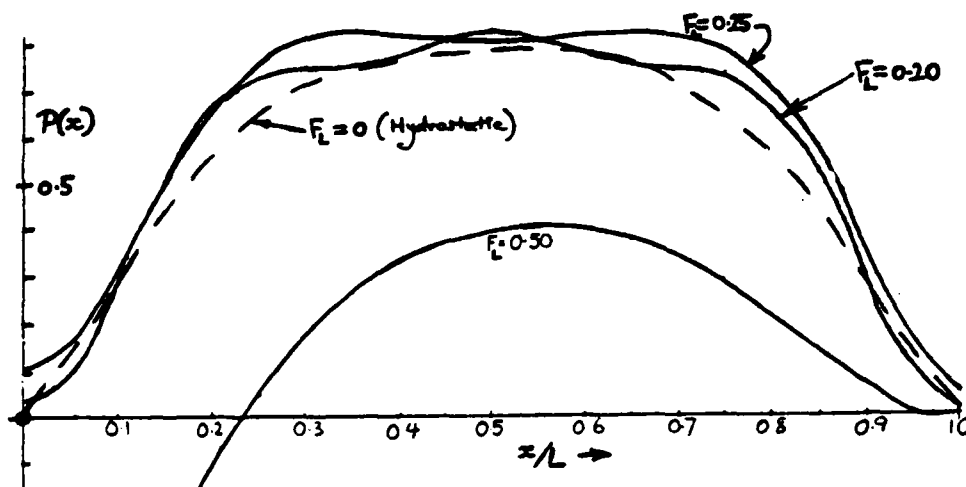


Figure 5-4. Free surface below symmetric curved body.

#### References for Chapter 5.

GRUNDY, I. and TUCK, E.O., "Airfoils moving in air close to a dynamic water surface", *paper in preparation*, 1984.

SELVADURAI, A.P.S., "Elastic Analysis of Soil-Foundation Interaction", 1970, Elsevier.

TUCK, E.O., "On air flow over free surfaces of stationary water", *Journal of the Australian Mathematical Society, Series B*, 19 (1975) 66-80.

TUCK, E.O., "Linearised planing-surface theory with surface tension. Part I: Smooth detachment." *Journal of the Australian Mathematical Society, Series B*, 23 (1982) 241-258.

TUCK, E.O., "A simple one-dimensional theory for air-supported vehicles over water", *Journal of Ship Research*, *in press*, 1984.

WEHAUSEN, J.V. and LAITONE, E.V., "Surface waves", in *Handbuch der Physik*, 9 (ed. W. Flugge) 1960, Springer-Verlag : Berlin.